FAIRSEA (ID 10046951)

"Fisheries in the AdriatIc Region - a Shared Ecosystem Approach"

D 4.1.2 – Scenario analysis of future circulation

Work Package:	WP4 **Implementation of a shared and integrated platform** Activity: 4.1 - **HYDRO – Hydrodynamic circulation and connectivity**
Type of Document	A report and a database on the distribution of temperature, salinity and velocity at different vertical layers, in the 21st century under emission scenarios RCP4.5 and RCP8.5
Use	[choose among: Public, Internal, Restricted to:]
Responsible PP	OGS
Authors	Stefano Querin (SQ), Marco Reale (MR)
Version and date	Version 1, 08/01/2021

Deliverable 4.1.2

Scenario analysis of future circulation

FAIRSEA – Fisheries in the Adriatic Region – a shared Ecosystem Approach

FAIRSEA is financed by Interreg V-A IT-HR CBC Programme (Priority Axis 1 – Blue innovation)

Start date: 01 January 2019
End date: 28 February 2021

Contents

Acronyms used

BFM	Biogeochemical Flux Model
CMCC	Centro Euro-Mediterraneo per i Cambiamenti Climatici
DIC	Dissolved Inorganic Carbon
DIN	Dissolved Nitrogen
EAF	Ecosystem Approach to Fisheries
EAFM	Ecosystem Approach to Fisheries Management
FAIRSEA	Fisheries in the Adrlatic Region – a Shared Ecosystem Approach
GSA	FAO Geographical Sub Areas
KoM	Kick-off Meeting
MFS	Mediterranean Forecasting System
NEMO	Nucleous for European Modelling of the Ocean
NetCDF	Network Common Data Form
OGS	Istituto Nazionale di Oceanografia e di Geofisica Sperimentale
OGSTM	OGS - Transport Model
PFT	Plankton Functional Types
WP	Work packages

Introduction

This report presents a description of the physical properties of the Adriatic and Ionian basins in the 21st century under emission scenarios RCP4.5 and RCP8.5 (IPCC, 2014: AR5). The future projections of hydrodynamic conditions are integrated by biogeochemical projections described in the companion report D 4.2.2. The analysis is based on two datasets, spanning the 2005-2100 time period, provided by the offline coupling between the physical MFS16 (Oddo et al., 2009; Cavicchia et al., 2011) and the transport-biogeochemical OGSTM-BFM (Lazzari et al., 2012; 2016; Cossarini et al., 2015) models. Results of the scenario simulations cover the entire Mediterranean Sea and have a spatial resolution of 1/16° in the horizontal direction, while the vertical discretization considers 70 unevenly-spaced levels. The datasets have been produced by using the computational resources available at the CINECA supercomputing center (www.cineca.it). Data and figures of the present deliverable have been, respectively, reprocessed and generated specifically for the Adriatic and Ionian basins.

The evolution of the physical conditions in the 21st century under the proposed scenarios integrates analysis of the present-day conditions provided in deliverable 4.1.1. Given the consistency of the models and the domain of both the reanalysis and scenario simulations, the anomalies provided in the present report can be combined (summed) to the mean values of the present-day condition (provided in D 4.1.1) to obtain the projected values of the physical variables in the 21st century.

The MFS16/OGSTM-BFM modelling system

The present deliverable describes the MFS16/OGSTM-BFM physical-biogeochemical modelling system and focuses on the projections of the hydrodynamic conditions in the 21st century under the emission scenarios RCP4.5 and RCP8.5. The biogeochemical projections are presented in the companion deliverable D 4.2.2.

The integrated physical-biogeochemical dataset covers the period 2005-2100. Data have a spatial resolution of 1/16°, which satisfies the requirements of the other WPs relying on hydrodynamic/biogeochemical output fields. Model domain is composed of 70 unevenly-spaced vertical levels at the depth of (from surface to bottom, in meters): 1.5, 4.6, 8.0, 11.6, 15.5, 19.6, 24.1, 29.0, 34.2, 39.7, 45.7, 52.2, 59.1, 66.4, 74.4, 82.9, 92.0, 102, 112, 124, 136, 148, 162, 177, 193, 210, 228, 247, 268, 290, 313, 339, 366, 395, 426, 458, 494, 532, 572, 615, 661, 710, 763, 819, 878, 943, 1011, 1084, 1162, 1245, 1334, 1428, 1529, 1637, 1751, 1874, 2004, 2143, 2291, 2448, 2616, 2795, 2985, 3187, 3402, 3631, 3874, 4132, 4406, 4698.

The integrated dataset includes monthly fields of fourteen 3D variables and three 2D variables. Three dimensional variables are temperature, salinity, meridional and zonal currents, chlorophyll-a, nitrate, phosphate, dissolved oxygen, phytoplankton carbon biomass, pCO_2, alkalinity, pH and net primary production. The two dimensional variables are sea surface height, bottom values of temperature and bottom values of oxygen.

The hydrodynamic data are produced by means of two climate simulations derived from the Mediterranean Forecasting System (MFS16, Oddo et al., 2009, Cavicchia et al., 2015), which is based on the hydrodynamic model NEMO (Nucleous for European Modelling of the Ocean). The biogeochemical data are produced by the OGSTM-BFM modeling system, which is based on the transport model OGSTMv2.0 and the

biogeochemical reactor Biogeochemical Flux Model BFMv5 (Lazzari et al., 2012, 2016; Cossarini et al., 2015, and references therein).

The Mediterranean Physical System

The physical MFS16 system is based on the NEMO (Nucleus for European Modelling of the Ocean - Ocean Parallelise) version 3.2 and 3.4 (Madec et al 1998). The MFS16 domain covers the whole Mediterranean Sea and part of the Atlantic Ocean with a horizontal grid resolution of 1/16 of degree. The MFS16 model computes the air-sea fluxes of water, momentum and heat using specific bulk formulae tuned for the Mediterranean Sea (see details in Oddo et al., 2009) and applied to the results of the atmospheric model CMCC-CM (extensively described in Scoccimarro et al., 2011). Moreover, a bias correction is applied to the atmospheric fields based on a 3-step procedure that uses the ERA-Interim dataset (Dee et al., 2011). The three steps are: re-gridding of ERA-interim fields on the CMCC-CM grid, computation of monthly biases between CMCC-CM model and ERA-Interim reanalysis for the present condition and, finally, addition of the biases to the original fields produced by the climate model. Further details on initial and boundary conditions, and set up of the MFS16 simulation are provided in Table 1. In particular, MFS16 adopts an open boundary at the Gibraltar strait with physical variables (zonal/meridional component of velocity, temperature and salinity) provided by the ocean compartment of the CMCC-CM modeling system. The riverine freshwater discharges and fluxes at the Dardanelles Strait were obtained from the hydrological component of the AOGCM used within the CIRCE project (based on the A1B scenario, Gualdi et al., 2013). The initial conditions of the Mediterranean Sea were obtained from the gridded temperature and salinity data produced by the SeaDataNet infrastructure (http://www.seadatanet.org/).

Model	MFS16 (Oddo et al.,2009) based on NEMO
Horizontal resolution	1/16° (Oddo et al.,2009)
Vertical Resolution	70 unevenly-spaced vertical levels (Oddo et al.,2009)
Time Step	540 s
Configuration	Hydrostatic
Initial conditions	Climatology (T,S) from regridding of the SeaDataNet data (http://www.seadatanet.org/).
Lateral boundary conditions	CMCC-CM (Scoccimarro et al.,2011)
River runoff	Rivers and Dardanelles runoff from the Circe project (Gualdi et al., 2013)
Horizontal diffusion	Bilaplacian (Oddo et al.,2009)
Vertical mixing	Based on Richardson number (Oddo et al.,2009)
Spin-up period	7 years

Table 1 - Setup and parameters used in the MSF16 simulation

The Mediterranean Biogeochemistry System

The biogeochemical modelling system is based on the OGSTMv2.0 and BFM5 models (Lazzari et al., 2010, 2012, 2016; Teruzzi et al., 2013; Cossarini et al., 2015, and references therein). The OGSTM model is a modified version of the OPA 8.1 transport model (Foujols et al., 2000), which computes the advection, the vertical diffusion and the sinking terms of the tracers (biogeochemical variables). OGSTM is driven by horizontal and vertical current velocities, vertical eddy diffusivity, potential temperature, and salinity, in addition to surface data for solar shortwave radiation and wind stress. These forcing fields are provided to OGSTM by the MFS16 System with daily frequency.

The features of the biogeochemical reactor BFM (Biogeochemical Flux Model) have been chosen to target the energy and mass fluxes through both the “classical food chain” and “microbial food web” pathways (Thingstad and Rassoulzadegan, 1995), and to consider co-occurring effects of multi-nutrient interactions. Both these factors are very important in the Mediterranean Sea, where microbial activity fuels the trophodynamics of a large part of the system, for much of the year, and both phosphorus and nitrogen can play limiting roles (Krom et al., 1991; Bethoux et al., 1998). The model presently includes four plankton functional types (PFTs: diatoms, flagellates, picophytoplankton and dinoflagellates), carnivorous and omnivorous mesozooplankton, bacteria, heterotrophic nanoflagellates and microzooplankton. The BFM model describes the biogeochemical cycles of 4 chemical compounds: carbon, nitrogen, phosphorus and silica through the dissolved inorganic, living organic and non-living organic compartments. BFM is also coupled to a carbonate system model (Cossarini et al., 2015), which consists of two prognostic state variables: alkalinity (ALK) and dissolved inorganic carbon (DIC) and two diagnostic variables: pH and pCO2. The non-living compartments consist of 3 groups: labile, semilabile and refractory organic matter. The last two are described in terms of carbon, nitrogen, phosphorus and silicon content.

The temporal scheme of OGSTM-BFM is an explicit forward-in-time scheme for the advection and horizontal diffusion terms, whereas an implicit time step is adopted for the vertical diffusion. The sinking term is a vertical flux, which acts on a sub-set of the biogeochemical variables (particulate matter and phytoplankton groups). Sinking velocity is fixed for particulate matter and it depends on nutrient availability for two phytoplankton groups (diatoms and dinoflagellates). Additional details on the biogeochemical model setup (initial, boundary and forcing conditions) are provided in Table 2 and described in the deliverable 4.2.2, which focus specifically on the biogeochemical future projections.

Model	OGSTM-BFM (Lazzari et al., 2012)
Horizontal resolution	1/16°
Vertical Resolution	70 unevenly-spaced vertical levels
Time Step	1800 s
Initial conditions	Climatology (nutrient/carbonate system variables) from EmodNET (Emodnet, 2018) and other datasets (Salon et al., 2019; Cossarini et al., 2015; Lazzari et al., 2016).
Lateral boundary conditions in Atlantic Ocean	Climatology (nutrient/carbonate system variables) from EmodNET (Emodnet, 2018) and other datasets (Salon et al., 2019; Cossarini et al., 2015)
River runoff	Rivers and Dardanelles input of nutrients from the Perseus project
Horizontal diffusion	Bilaplacian
Vertical mixing	Implicit scheme
Spin-up period	100 years, used as control run

Table 2 - Setup and parameters used in the OGSTM-BFM simulation

IPCC future scenarios

Two future emission scenarios, RCP4.5 and RCP8.5 (Moss et al., 2010), are used to force the atmospheric compartment of the CMCC-CM model and, subsequently, the coupled physical-biogeochemical MFS16-OGSTM-BFM model of the Mediterranean Sea. In particular, the RCP4.5 represents an intermediate scenario where CO2 emissions peak around 2040 (causing the maximum increase in CO2 concentration, Fig. 1), then decline (with a resulting plateau in the CO2 concentration). As a consequence, at the end of the 21st century, the atmospheric pCO_2 will be around 560-580 ppm (Fig.1) and atmospheric temperature will increase by 1.8 (1.1 to 2.6) °C with respect to the present-day condition. In the worst-case scenario RCP8.5, the CO_2 emissions will continue to rise throughout the 21st century, the pCO_2 concentration will rise to more than 1200 ppm (Fig. 1) at the end of the 21st century, and the temperature increase will be of 3.7 (2.6 to 4.8) °C (IPCC, 2014: AR5).

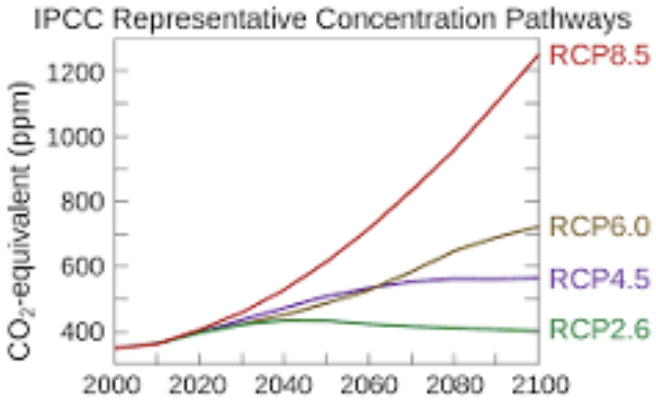

Figure 1 - Atmospheric pCO_2 concentration under different future scenarios used for the climate modeling of the IPCC fifth Assessment Report (From: https://en.wikipedia.org/wiki/Representative_Concentration_Pathway; data: IPCC, 2014 - AR5).

Methodology for the future scenario analysis

Following the CMIP protocol, the scenario analysis consists of a spin-up period and a 100-year-long simulation. The first 15 years of the simulation are used as a reference period for the present-day condition. Its average constitutes the baseline, which the simulated evolution is compared to, in order to evaluate the effect due to the climate scenario (Fig. 2).

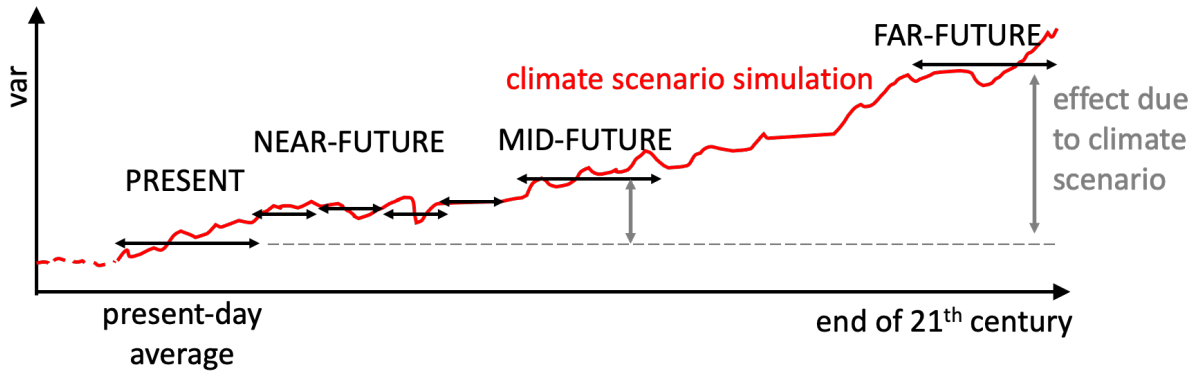

Figure 2 - Scheme of the analysis for the future scenario simulation: spin-up period (red dashed line),100-year simulation (red solid line), and time intervals for the temporal averages (horizontal solid black double-headed arrows).

In particular, considering the monthly output of the simulations, we computed the annual timeseries $X\_Evo_{SCEN,k}$ with k=2005, ..., 2099 for the following vertical averaged levels: 0-50 m, 50-100 m, 100-200 m, 200-500 m and 500-800 m. Then we selected the following period: 2005-2020 (hereafter PRESENT), 2040-2059 (hereafter MID-FUTURE) and 2080-2099 (hereafter FAR-FUTURE). Additionally, short 5-year periods of the next three decades include 2021-2025, 2026-2030, 2031-2035, 2036-2040 time windows (hereafter NEAR FUTURE). To point out for each period the variation of each variable with respect to the PRESENT we define the quantity X_ANOM_{period}. More specifically being the period

for example MID-FUTURE or FAR-FUTURE (both will be discussed in this deliverable) we defined $X\_ANOM_{MID\text{-}FUTURE}$ and $X\_ANOM_{FAR\text{-}FUTURE}$ as:

$$X\_ANOM_{MID\text{-}FUTURE} = Evo_{X\_SCEN\text{-}MID\text{-}FUTURE} - Evo_{X\_SCEN\text{-}PRESENT} \quad (1)$$

$$X\_ANOM_{FAR\text{-}FUTURE} = Evo_{X\_SCEN\text{-}FAR\text{-}FUTURE} - Evo_{X\_SCEN\text{-}PRESENT} \quad (2)$$

Where $Evo_{X\_SCEN\text{-}MID\text{-}FUTURE,}$ $Evo_{X\_SCEN\text{-}FAR\text{-}FUTURE}$ and $Evo_{X\_SCEN\text{-}PRESENT}$ is the average $Evo_{X\_SCEN,k}$ for the MID-FUTURE, FAR-FUTURE and PRESENT time period, respectively (Figure 2). Hereafter, if not differently specified, all the mean variables shown later in the maps will be represented by X_ANOM.

The analysis of the future scenario is integrated by the time series of the annual anomalies computed as:

$$\langle X\_ANOM_k \rangle = \langle Evo_{SCEN,k} \rangle - \langle Evo_{SCEN\text{-}PRESENT} \rangle \quad (3)$$

where < > represents the spatial average calculated over the three GSA areas and the inshore (areas shallower than 200 m) and off-shore (areas deeper than 200 m) zones.

It is worth to note that the climate scenario anomalies (timeseries and reference period maps presented in the next sections) can be used conjunctly with the assessment of the present-day condition (deliverable D 4.1.1) to eventually reconstruct the future actual values of the hydrodynamic variables. Indeed, given the consistency of the models domain configuration between reanalysis (deliverable D 4.1.1) and climate simulations (present deliverable), the layers of the future scenario anomalies can be directly combined with the layers of the present-day average conditions in the FAIRSEA web portal.

Physical properties of the Adriatic Sea and northern Ionian Sea (GSA 17-18-19) in the future climate scenarios

In this section we analyze the spatial patterns and temporal behavior of the physical properties in the Adriatic and Ionian systems in the future climate under emission scenarios RCP4.5 and RCP8.5, with a specific focus on the period 2040-2059 (MID-FUTURE) and 2080-2099 (FAR-FUTURE). The consistency of the models (except for the data assimilation in the reanalysis) and the configuration of the domain and boundaries used in the reanalysis (D 4.1.1) and in the climate simulations ensures that the differences and anomalies are mainly driven by the changes in the atmospheric forcing and Atlantic boundary that characterize the future evolution of the climate in the Mediterranean region.

Temperature

Figures 3 and 4 show the mean annual anomalies of temperature for the MID-FUTURE period, with respect to PRESENT, under the emission scenarios RCP4.5 and RCP8.5, respectively. The FAR-FUTURE anomalies for the two scenarios are shown in Figures 5 and 6. The distribution of temperature anomalies shows a substantial and uniform warming of the water column in both basins, which is more marked at the end of the century in the RCP8.5 scenario. The evolution and pattern of the water column warming are well correlated to the atmospheric temperature rise in response to the increase in greenhouse gases concentration. The time-series of the mean spatial temperature anomalies for inshore (Fig. 7) and offshore (Fig. 8) areas in RCP4.5 (left panel) and RCP8.5 (right panel) scenarios are shown for the three GSA areas: northern Adriatic (GSA17), southern Adriatic (GSA18) and Ionian (GSA19). While the two scenarios show a comparable evolution of the temperature increase during the first part of 21th century, the warming related to RCP8.5 is stronger in the second part of the century. The mean

temperature anomalies can be on the order of 3-4°C in the surface and subsurface layers of both inshore and offshore zones, and 1-2°C in the deeper layers. Considering the bottom of the water column (Fig. 9, 10, 11 and 12), it becomes evident that the shallower areas will be more affected by the warming. Since the intensity of the warming is maximum at surface and progressively, and almost linearly, decreases with depth, the northern Adriatic (GSA17) and the inshore areas of southern Adriatic present the highest increase of the bottom temperature. Among the two scenarios, the RCP8.5 presents the worst impact, with an increase of 3-4°C of the bottom temperature in the coastal areas by the end of the century.

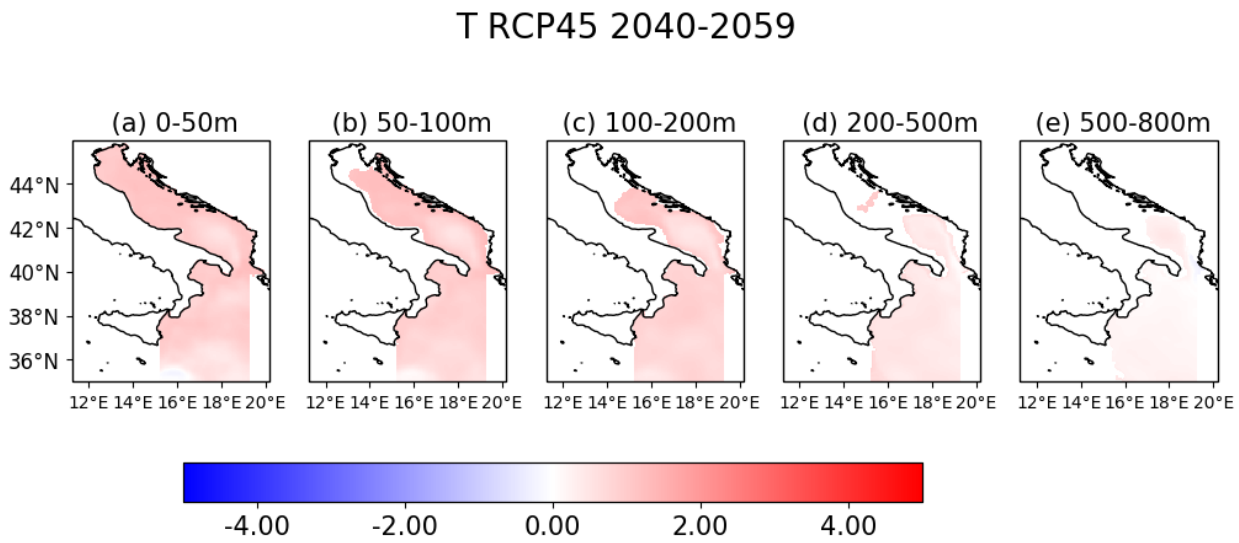

Figure 3 - Mean temperature anomaly (°C) in the MID-FUTURE of the RCP4.5 scenario in the five layers: 0-50 m, 50-100 m, 100-200 m, 200-500 m and 500-800 m.

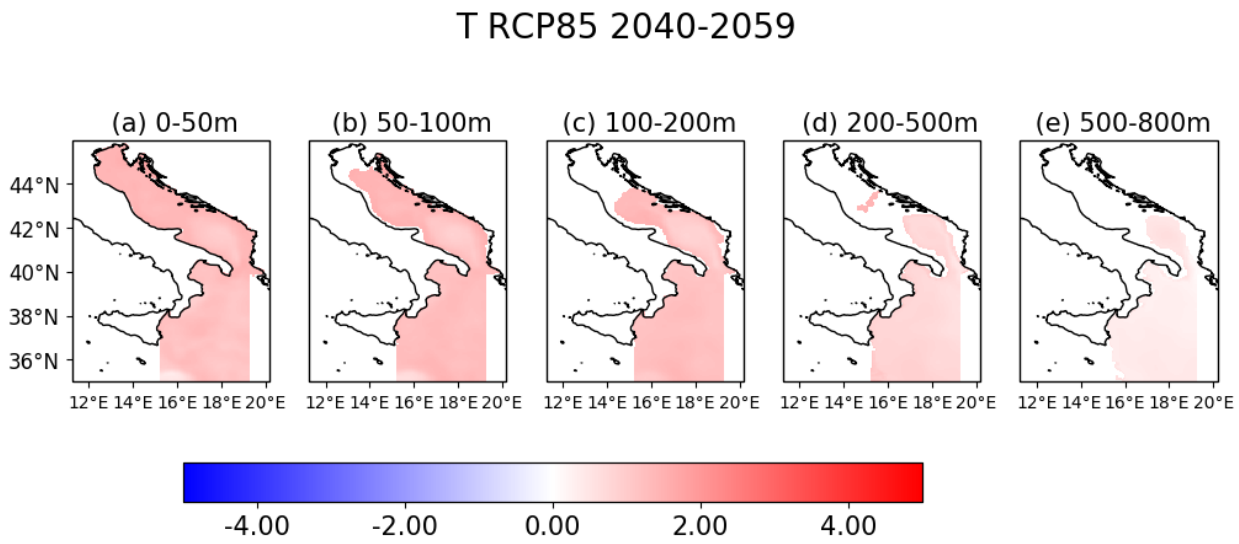

Figure 4 - Mean temperature anomaly (°C) in the MID-FUTURE of the RCP8.5 scenario in the five layers: 0-50 m, 50-100 m, 100-200 m, 200-500 m and 500-800 m

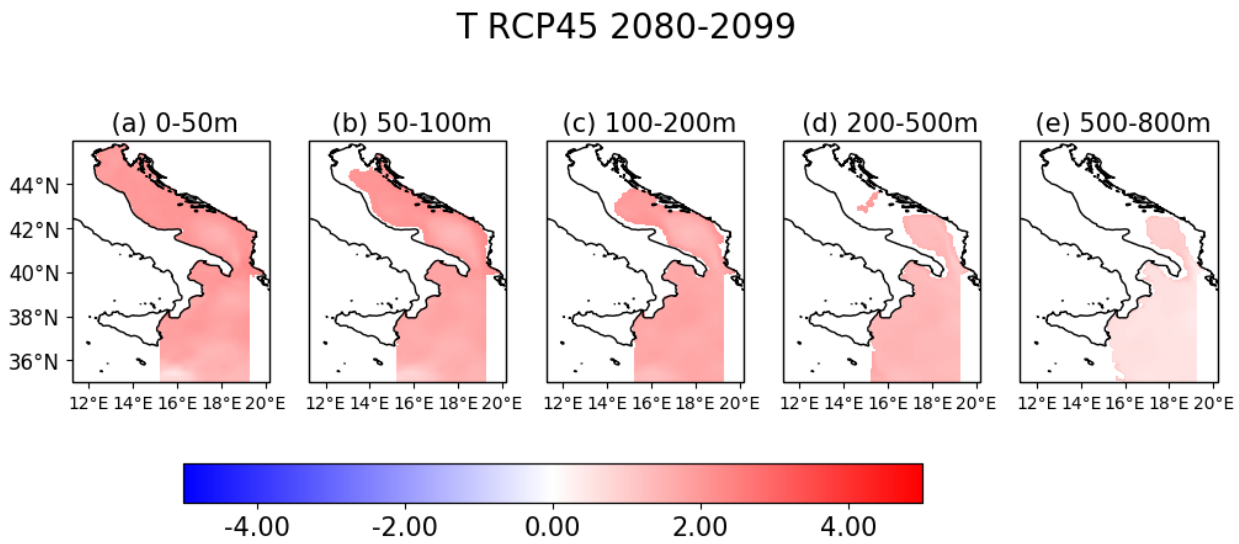

Figure 5 - Mean temperature anomaly (°C) in the FAR-FUTURE of the RCP4.5 scenario in the five layers: 0-50 m, 50-100 m, 100-200 m, 200-500 m and 500-800 m

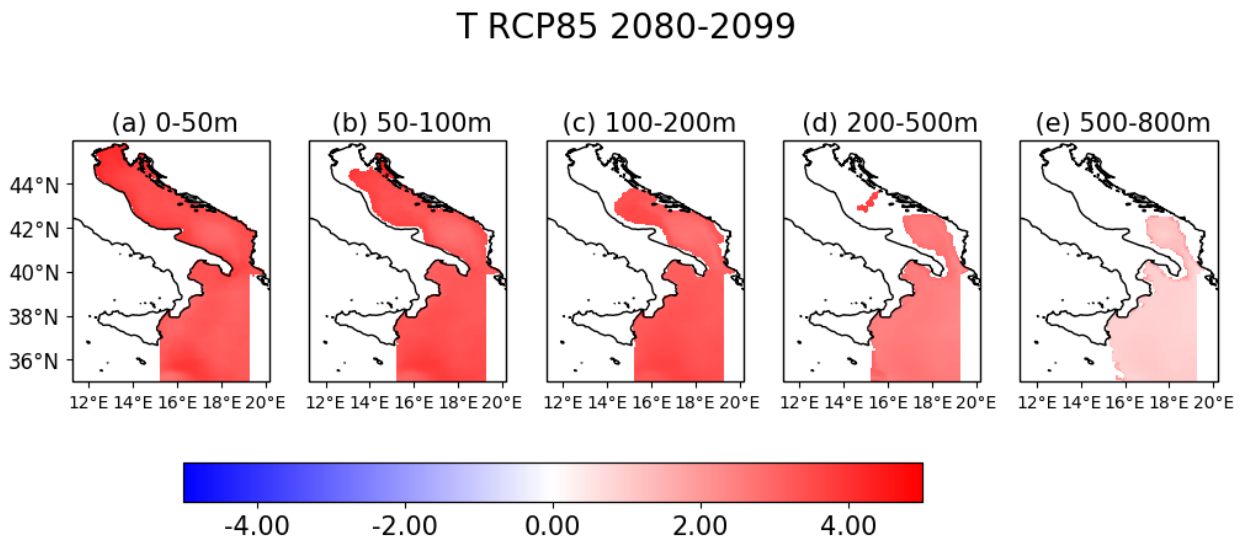

Figure 6 - Mean temperature anomaly (°C) in the FAR-FUTURE of the RCP8.5 scenario in the five layers: 0-50 m, 50-100 m, 100-200 m, 200-500 m and 500-800 m

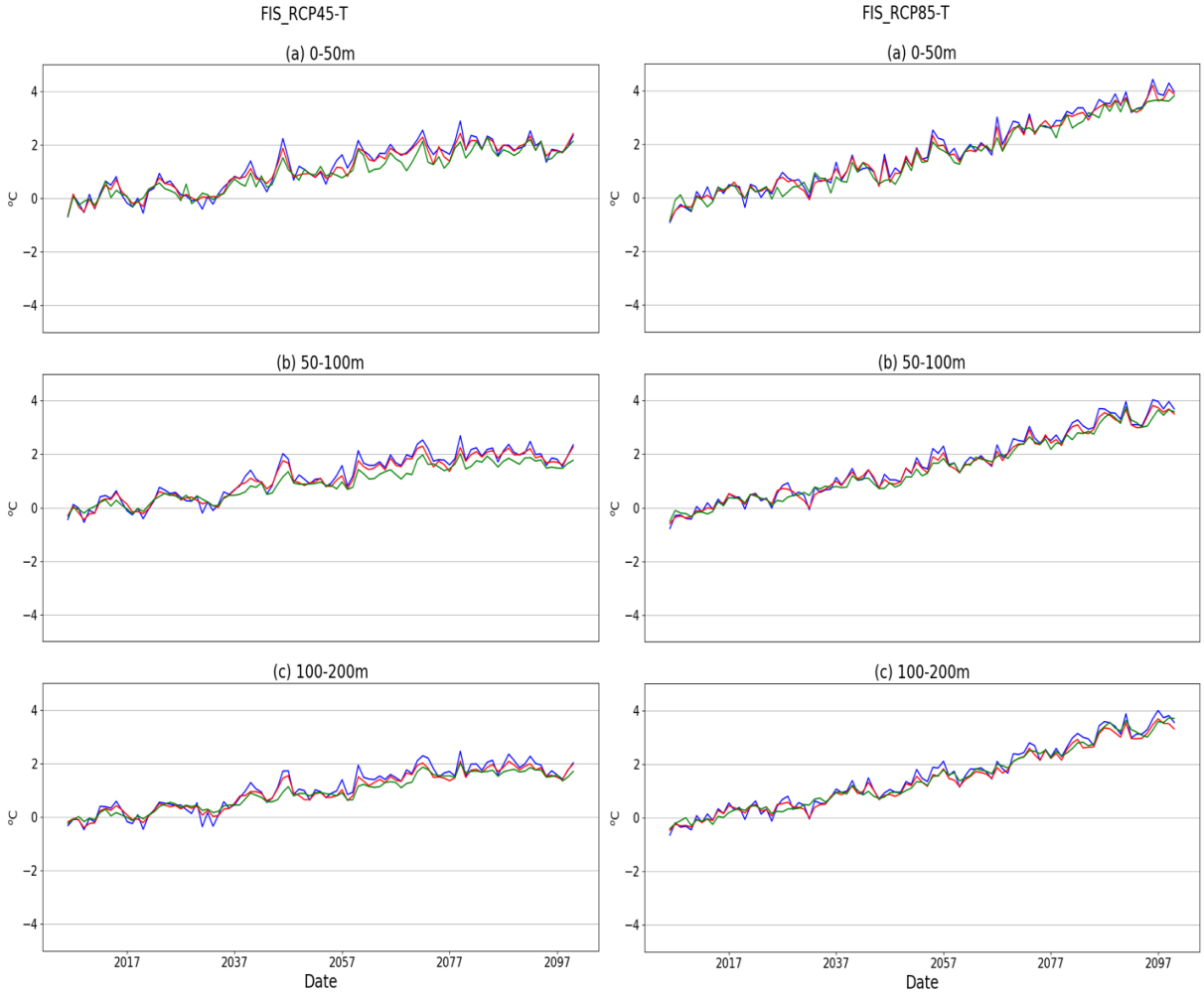

Figure 7 - Annual time series of temperature anomaly (°C) in the three inshore (depth less than 200 m) areas of the Adriatic-Ionian Sea: GSA17 - northern Adriatic (blue), GSA18 - southern Adriatic (red) and GSA19 - Ionian (green). Time series cover the 2005-2099 period for the two emission RCP4.5 (left) and RCP8.5 (right) scenarios.

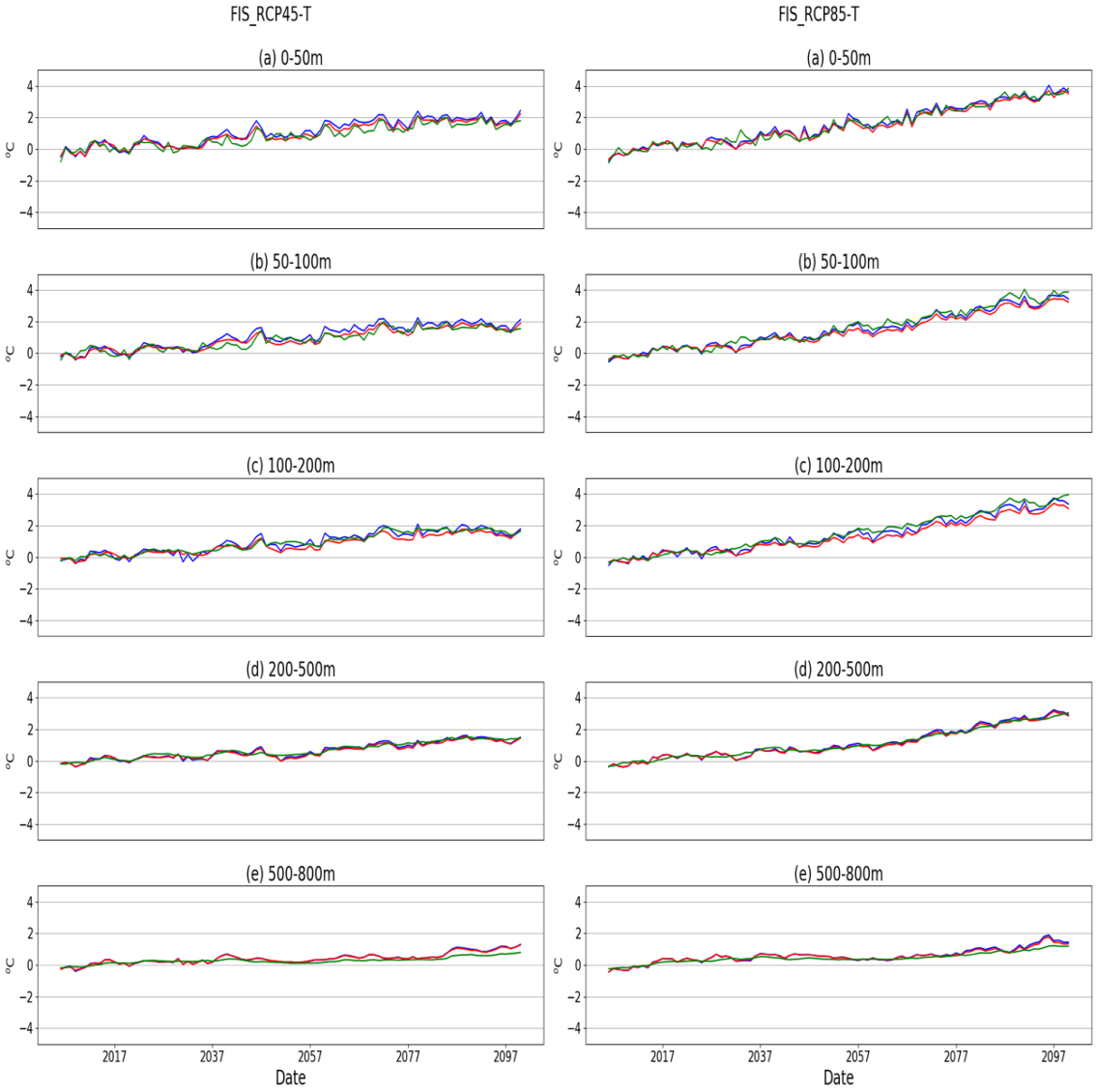

Figure 8 - Annual time series of temperature anomaly (°C) in the three offshore (deeper than 200 m) areas of the Adriatic-Ionian Sea: GSA17 - northern Adriatic (blue), GSA18 - southern Adriatic (red) and GSA19 - Ionian (green). Time series cover the 2005-2099 period for the two emission RCP4.5 (left) and RCP8.5 (right) scenarios.

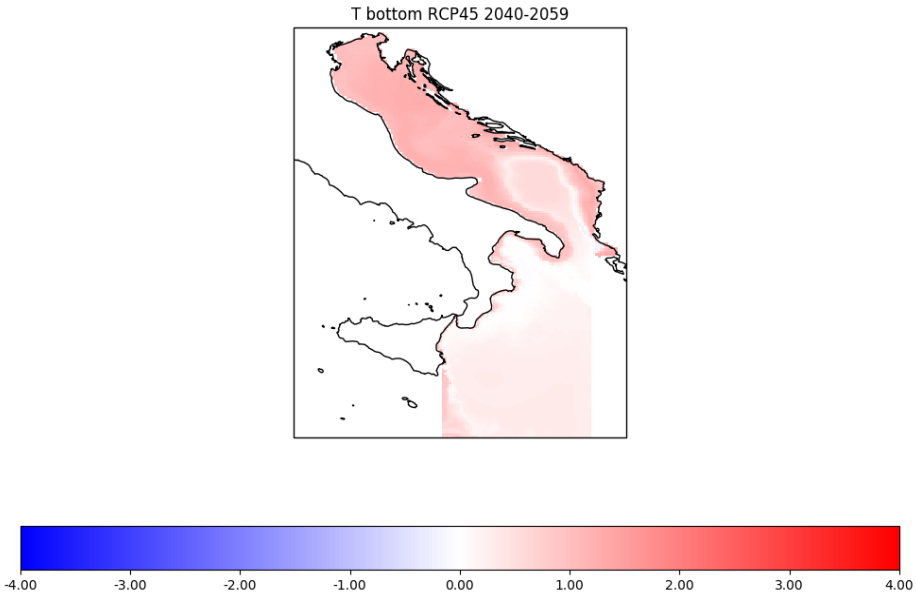

Figure 9 - Mean temperature anomaly (°C) at the bottom in the MID-FUTURE of the RCP4.5 scenario.

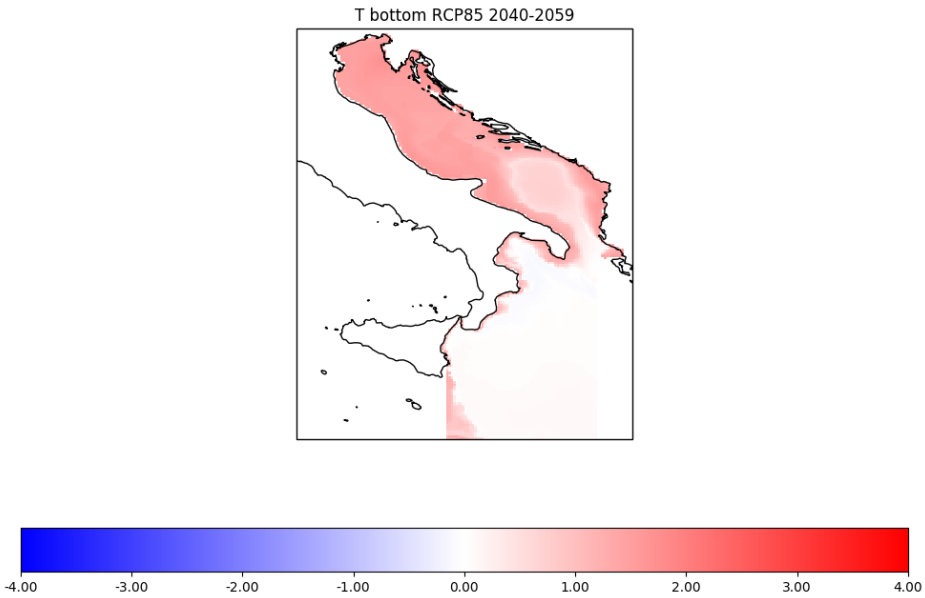

Figure 10 - Mean temperature anomaly (°C) at the bottom in the MID-FUTURE of the RCP8.5 scenario.

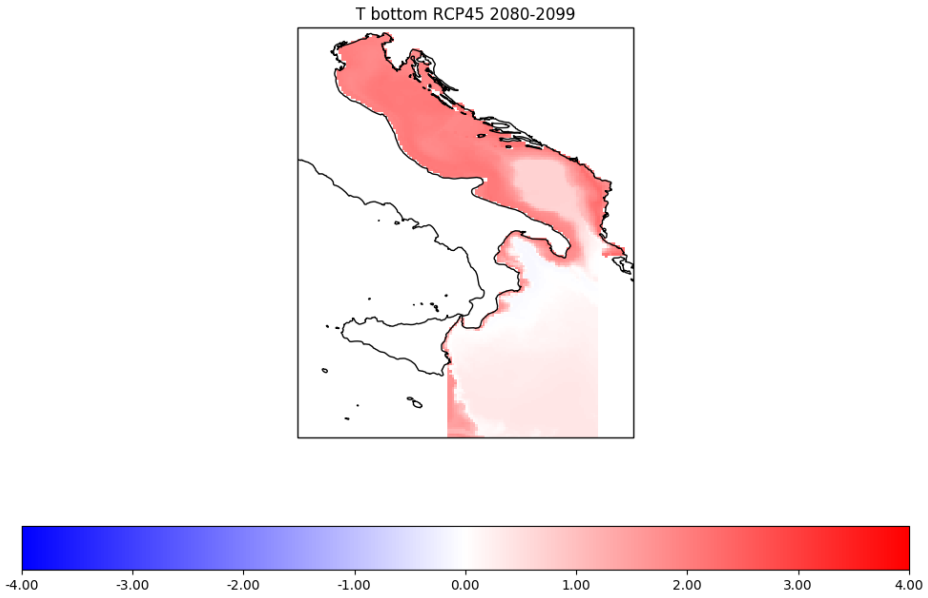

Figure 11 - Mean temperature anomaly (°C) at the bottom in the FAR-FUTURE of the RCP4.5 scenario.

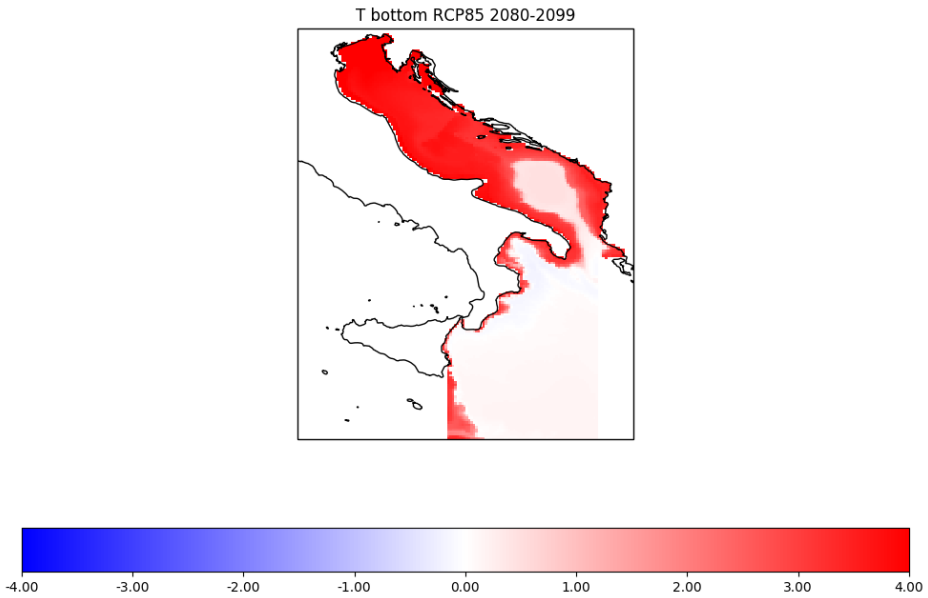

Figure 12 - Mean temperature anomaly (°C) at the bottom in the FAR-FUTURE of the RCP8.5 scenario.

Salinity

Salinity anomalies computed for the MID-FUTURE and FAR-FUTURE under the two emission scenarios are shown in the maps of Figs. 13-16. The salinity distribution in a basin usually reflects the effects of the freshwater balance (evaporation-precipitation-runoff), local circulation patterns and large-scale dynamics. A very slight decrease of surface salinity (less than 0.1) is reported in most of the investigated areas in the MID-FUTURE of the RCP4.5 scenario (Fig.13), and a marked decrease of salinity is shown in the southern part of the Ionian GSA area. On the other hand, an opposite pattern is observed in the RCP8.5 (Fig.14) scenario in the MID_FUTURE: almost all the surface Adriatic Sea shows a positive or neutral change, while the Ionian GSA is mostly characterized by a negative anomaly.

By the end of the century (FAR-FUTURE), both scenarios show an increase of salinity in the surface water of the Adriatic Sea, which is stronger in the RCP8.5 (Fig. 16). The salinity increase reflects the increase of the water budget (evaporation minus precipitation minus runoff, Fig. 6 in Gualdi et al., 2013) that affects more the coastal areas. On the other hand, both scenarios show a negative anomaly in the surface water of the Ionian Sea (especially in RCP8.5), which could be due to a possible change in the circulation pattern of the modified Atlantic waters.

Considering the subsurface and deep layers, RCP8.5 shows a substantial saltening of the water column in the FAR-FUTURE (Fig. 16), whereas the other maps (Fig. 13-15) show quite weak anomalies both positive and negative, which might simply reflect changes in water masses position and circulation patterns.

The time-series of the mean spatial salinity anomalies for inshore (Fig. 17) and offshore (Fig. 18) areas in RCP4.5 (left panel) and RCP8.5 (right panel) scenarios are shown for the three GSA areas: northern Adriatic (GSA17), southern Adriatic (GSA18) and Ionian

(GSA19). For RCP4.5 we do not observe a significant tendency in the salinity of three areas. On the other hand, for the RCP8.5 and more specifically for the inshore part of the Adriatic Sea a significant and stronger saltening of the waters is simulated throughout the 21st century.

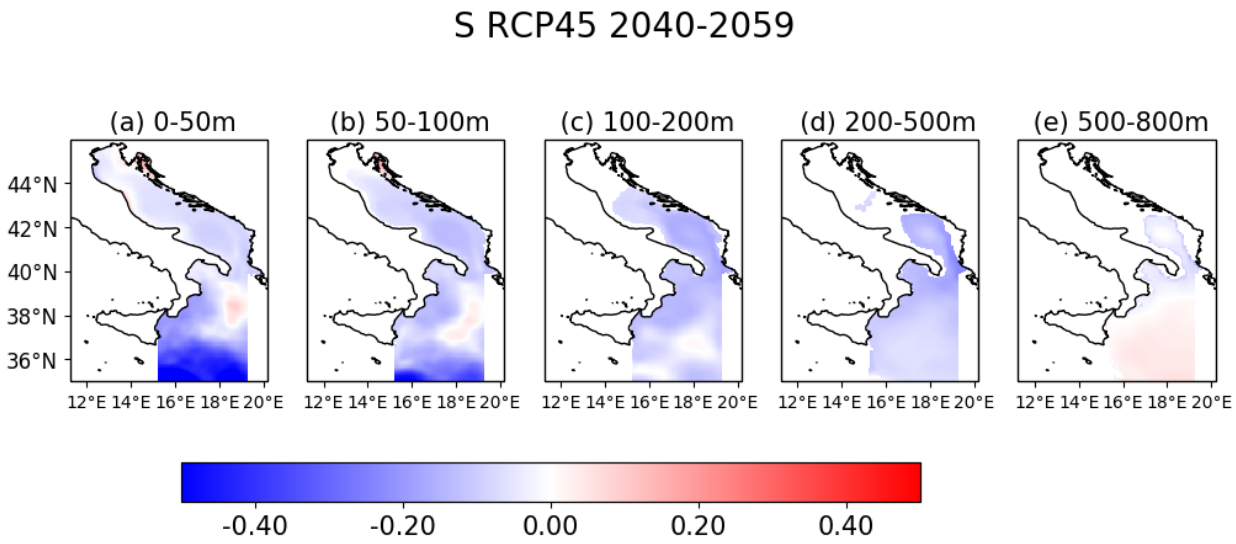

Figure 13 - Mean salinity anomaly in the MID-FUTURE of the RCP4.5 scenario in the five layers: 0-50 m, 50-100 m, 100-200 m, 200-500 m and 500-800 m.

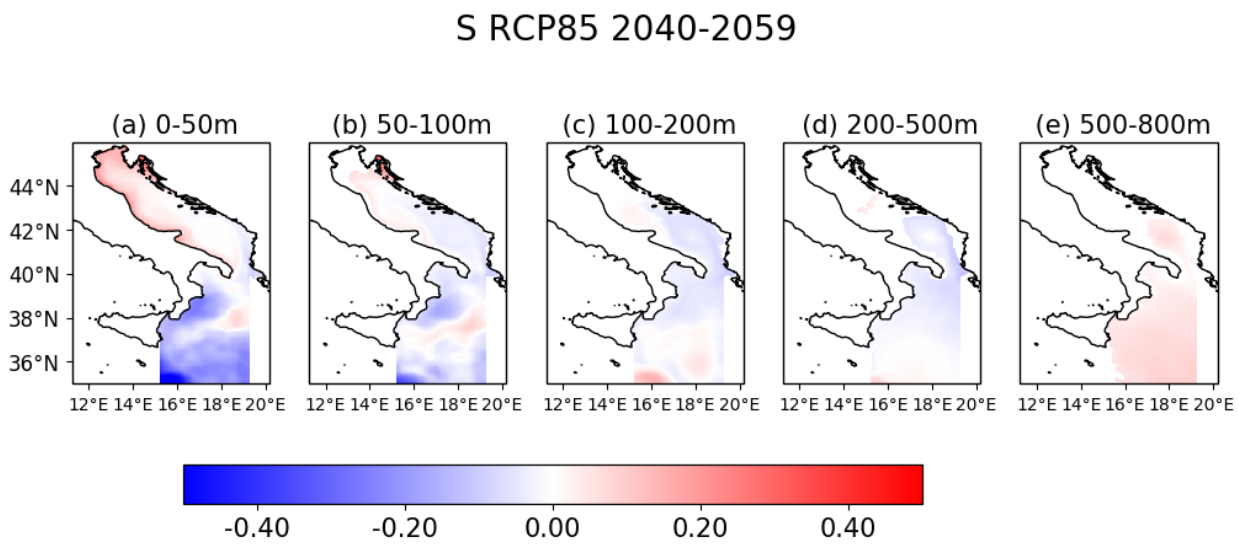

Figure 14 - Mean salinity anomaly in the MID-FUTURE of the RCP8.5 scenario in the five layers: 0-50 m, 50-100 m, 100-200 m, 200-500 m and 500-800 m.

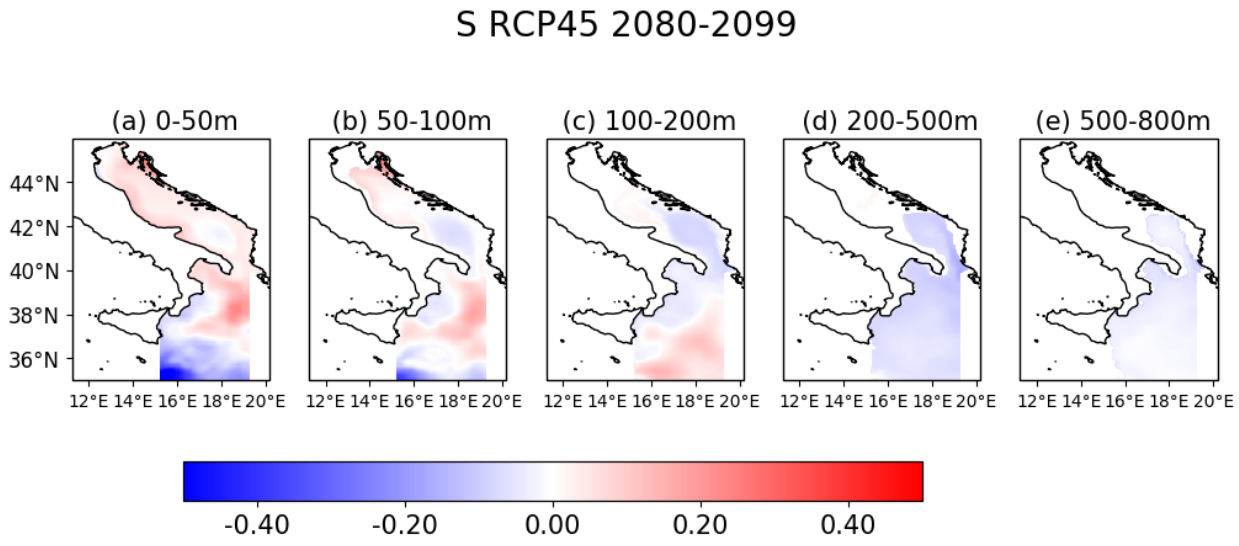

Figure 15 - Mean salinity anomaly in the FAR-FUTURE of the RCP4.5 scenario in the five layers: 0-50 m, 50-100 m, 100-200 m, 200-500 m and 500-800 m.

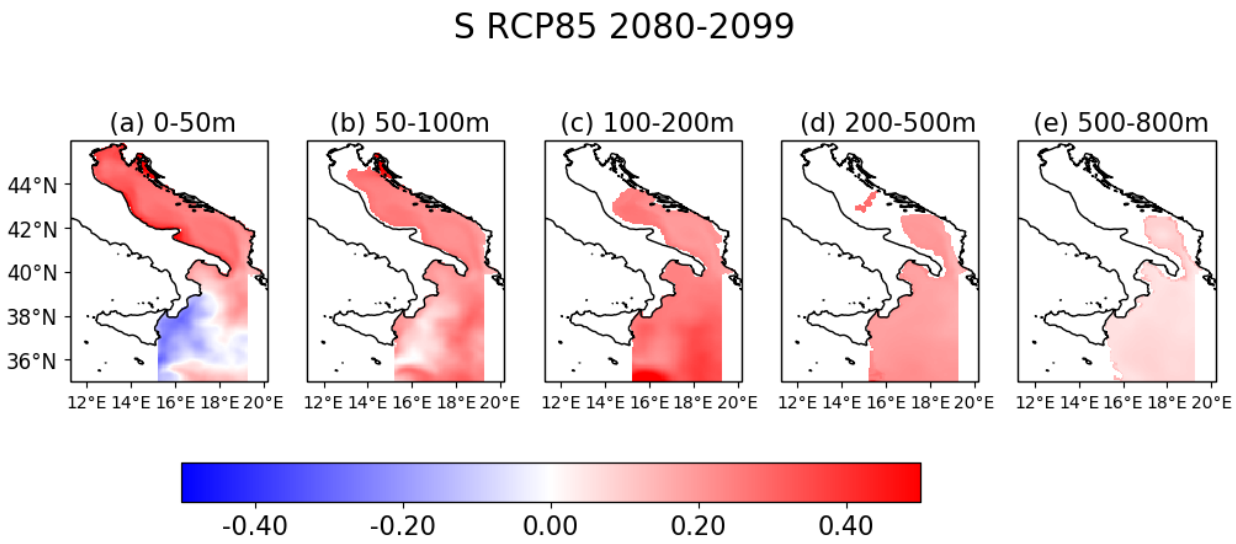

Figure 16 - Mean salinity anomaly in the FAR-FUTURE of the RCP8.5 scenario in the five layers: 0-50 m, 50-100 m, 100-200 m, 200-500 m and 500-800 m.

Figure 17 - Annual time series of salinity anomaly in the three inshore (depth less than 200 m) areas of the Adriatic-Ionian Sea: GSA17 - northern Adriatic (blue), GSA18 - southern Adriatic (red) and GSA19 - Ionian (green). Time series cover the 2005-2099 period for the two emission RCP4.5 (left) and RCP8.5 (right) scenarios.

Figure 18 - Annual time series of salinity anomaly in the three offshore (deeper than 200 m) areas of the Adriatic-Ionian Sea: GSA17 - northern Adriatic (blue), GSA18 - southern Adriatic (red) and GSA19 - Ionian (green). Time series cover the 2005-2099 period for the two emission RCP4.5 (left) and RCP8.5 (right) scenarios.

Connectivity: current streamlines and velocity intensity

Fig.19-20 show the mean annual kinetic energy (KE) and the streamlines of the velocity field for the present, mid and far-future periods, under emission scenario RCP4.5 and RCP8.5, respectively. The streamlines and KE for the present period show the existence of some strong features of the circulation in the three sub-areas of the Adriatic-Ionian domain, as the intense cyclonic circulation of the middle/southern Adriatic Pits, the intense northern Ionian Gyre and Mid-Ionian Jet, the velocity field connecting at different depths northern and southern Adriatic and southern Adriatic and Ionian Sea through the Strait of Otranto, the intense currents along the Italian Adriatic coast associated with a transport of relatively fresher waters from the northern Adriatic toward the Otranto strait. Under emission scenario RCP4.5, only small changes can be observed in the mean circulation of both basins. On the other hand, a slight weakening of the circulation in the southern Adriatic Pit is observed in the RCP8.5 scenario, which results in a higher stratification of the water column in the area.

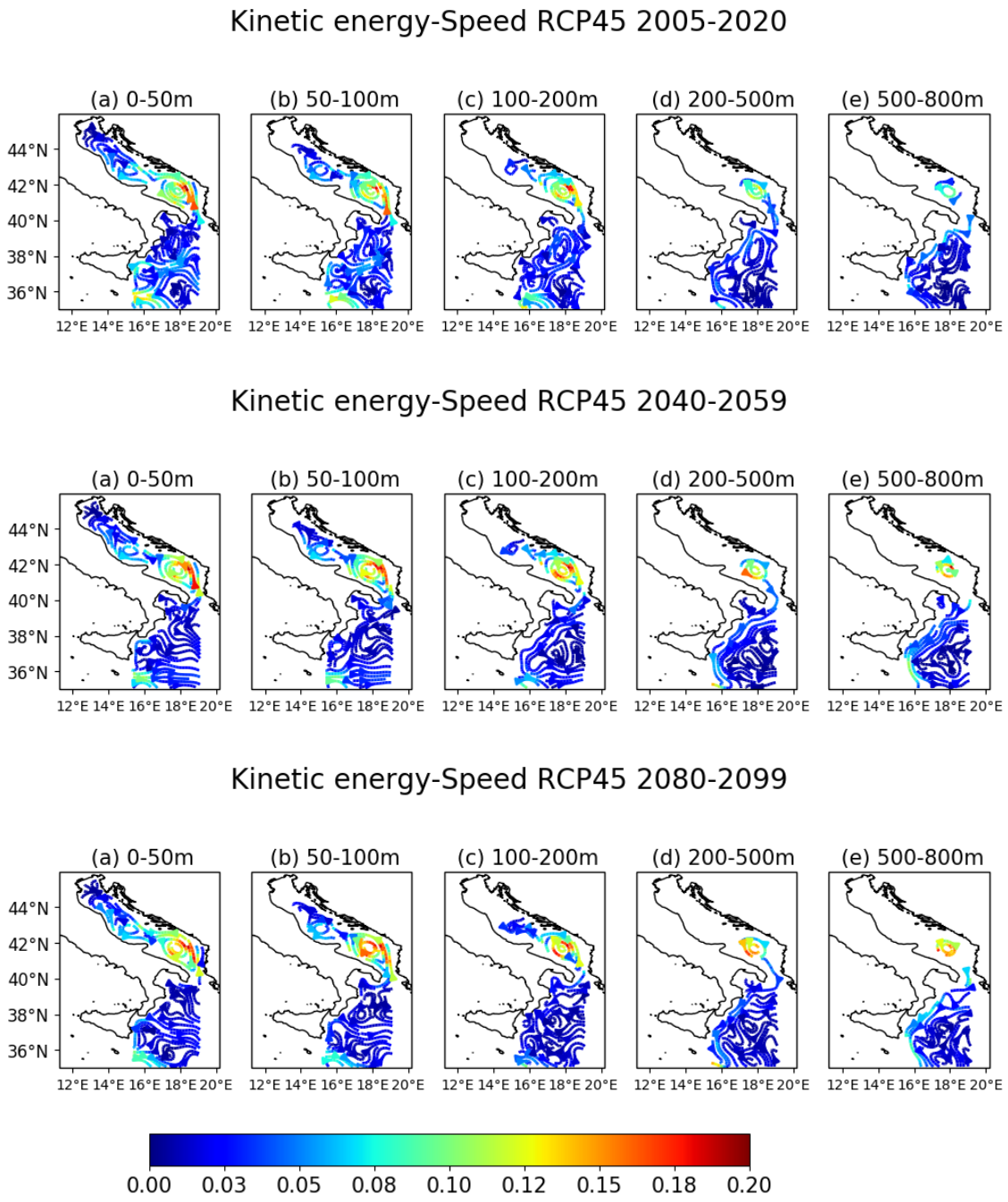

Figure 19 - Streamlines in the PRESENT (upper panel), MID-FUTURE (central panel) and FAR-FUTURE (bottom panel) periods between 0-50 m, 50-100 m, 100-200 m, 200-500 m and 500-800 m under emission scenario RCP4.5. The mean kinetic energy of the flow (m^2/s^2) is represented by the colour of the streamlines.

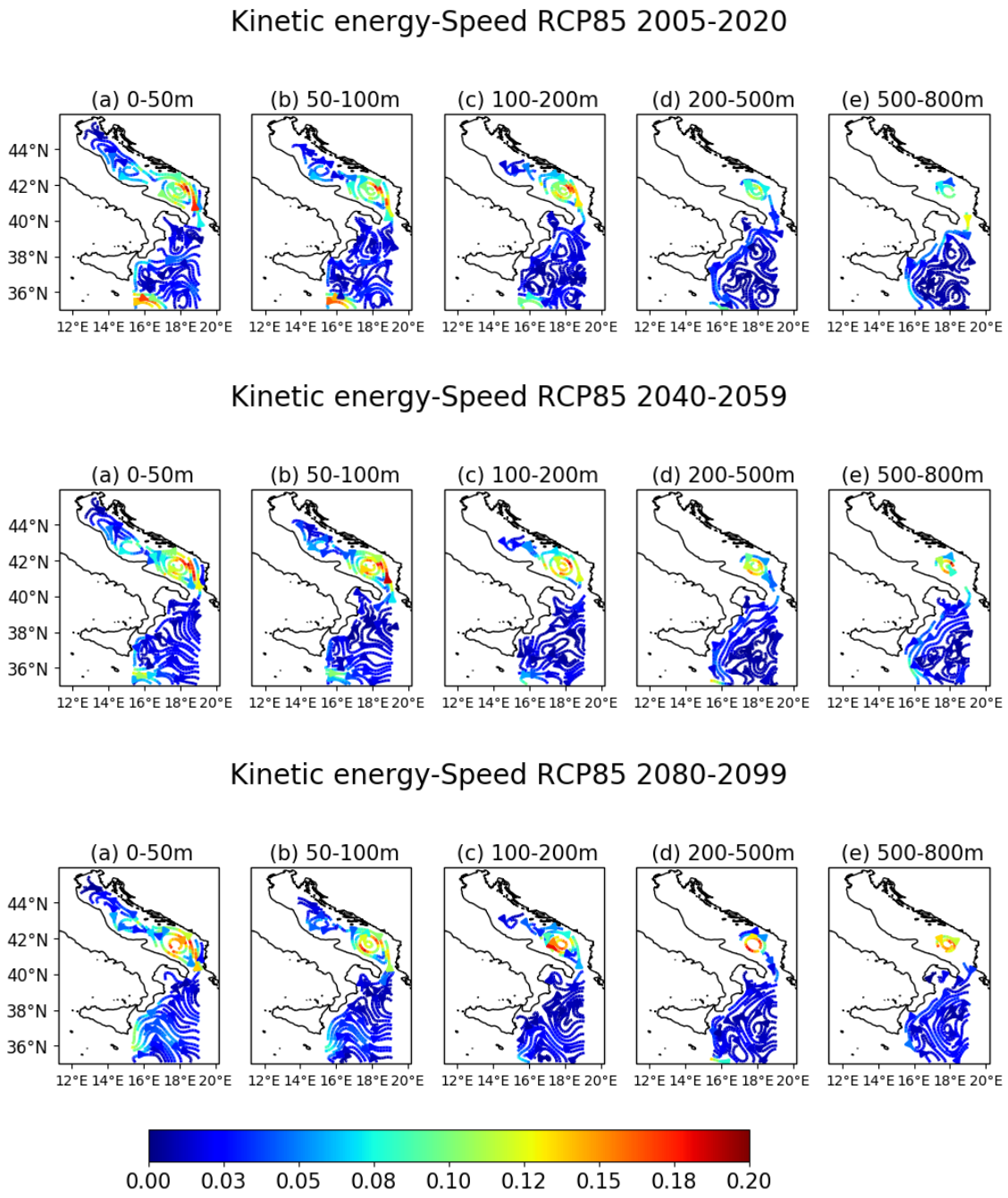

Figure 20 - Same as Figure 19 for emission scenario RCP8.5.

Near Future evolution of physical variables

Mean values of the physical variables for the 5-year intervals of the next two decades and for the MID-FUTURE and FAR-FUTURE periods are reported in the following tables.

T (°C)		PRESENT	2021 - 2025		2026 - 2030		2031 - 2035		2036 - 2040		2040 - 2059		2080 - 2099	
			RCP4.5	*RCP8.5*	RCP4.5	*RCP8.5*	RCP4.5	*RCP8.5*	RCP4.5	*RCP8.5*	RCP4.5	*RCP8.5*	RCP4.5	*RCP8.5*
ADR1	0 - 50 m	**16.37**	16.95	*16.67*	16.28	*17.05*	16.57	*16.92*	17.30	*17.47*	17.48	*17.78*	18.35	*20.00*
	50 - 100 m	**14.09**	14.65	*14.43*	14.27	*14.76*	14.34	*14.63*	15.11	*15.21*	15.26	*15.50*	16.11	*17.58*
	100 - 200 m	**13.55**	14.01	*13.84*	13.78	*14.11*	13.73	*14.01*	14.46	*14.60*	14.59	*14.86*	15.44	*16.88*
	200 - 500 m	**13.27**	13.61	*13.55*	13.38	*13.78*	13.23	*13.67*	13.95	*14.16*	13.94	*14.31*	14.84	*16.33*
	500 - 800 m	**13.55**	13.77	*13.86*	13.76	*14.08*	13.72	*13.86*	14.04	*14.20*	13.84	*14.05*	14.50	*14.92*
ADR2	0 - 50 m	**17.17**	17.66	*17.51*	17.23	*17.65*	17.35	*17.56*	17.96	*18.17*	18.07	*18.41*	19.04	*20.49*
	50 - 100 m	**14.63**	15.03	*14.98*	14.91	*15.10*	14.83	*15.05*	15.42	*15.58*	15.51	*15.81*	16.39	*17.73*
	100 - 200 m	**14.10**	14.43	*14.43*	14.40	*14.53*	14.28	*14.46*	14.80	*14.96*	14.82	*15.14*	15.69	*17.05*
	200 - 500 m	**13.83**	14.06	*14.14*	14.09	*14.27*	13.98	*14.10*	14.37	*14.48*	14.22	*14.57*	15.14	*16.43*
	500 - 800 m	**13.55**	13.78	*13.87*	13.75	*14.09*	13.72	*13.89*	14.04	*14.18*	13.85	*14.05*	14.46	*14.77*
ION	0 - 50 m	**18.71**	19.05	*18.88*	18.73	*19.06*	19.03	*19.35*	19.19	*19.53*	19.47	*19.86*	20.38	*21.98*
	50 - 100 m	**15.69**	16.08	*15.94*	15.97	*16.11*	15.99	*16.52*	16.13	*16.64*	16.49	*16.95*	17.30	*19.10*
	100 - 200 m	**14.89**	15.26	*15.22*	15.29	*15.20*	15.19	*15.57*	15.49	*15.97*	15.69	*16.12*	16.57	*18.24*
	200 - 500 m	**14.22**	14.59	*14.55*	14.61	*14.49*	14.49	*14.71*	14.76	*15.04*	14.69	*15.01*	15.62	*16.78*
	500 - 800 m	**13.71**	13.97	*13.96*	13.94	*14.04*	13.95	*14.11*	14.03	*14.20*	13.90	*14.08*	14.30	*14.67*

Table 3 - Mean values of temperature for the present condition (bold font), for the 5-year intervals of the next two decades and for the MID-FUTURE and FAR-FUTURE periods. For each time period in the future, both the RCP4.5 (normal font) and RCP8.5 (italic font) scenarios have been considered. Data have been subdivided into the three GSA areas: northern Adriatic (ADR1 - GSA17), southern Adriatic (ADR2 - GSA18) and Ionian (ION - GSA19). For each area, five layers with increasing depth (0-50 m, 50-100 m, 100-200 m, 200-500 m, 500-800 m) have been considered.

S		PRESENT	2021 - 2025		2026 - 2030		2031 - 2035		2036 - 2040		2040 - 2059		2080 - 2099	
			RCP4.5	*RCP8.5*	RCP4.5	*RCP8.5*	RCP4.5	*RCP8.5*	RCP4.5	*RCP8.5*	RCP4.5	*RCP8.5*	RCP4.5	*RCP8.5*
ADR1	0 - 50 m	**38.11**	38.20	*38.26*	38.24	*38.38*	38.19	*38.20*	38.24	*38.16*	38.07	*38.17*	38.16	*38.41*
	50 - 100 m	**38.51**	38.53	*38.63*	38.62	*38.70*	38.52	*38.56*	38.64	*38.55*	38.44	*38.52*	38.53	*38.77*
	100 - 200 m	**38.53**	38.55	*38.64*	38.63	*38.72*	38.53	*38.58*	38.65	*38.58*	38.44	*38.52*	38.52	*38.77*
	200 - 500 m	**38.62**	38.63	*38.71*	38.71	*38.82*	38.64	*38.67*	38.73	*38.68*	38.50	*38.60*	38.58	*38.85*
	500 - 800 m	**38.76**	38.79	*38.85*	38.83	*38.95*	38.82	*38.82*	38.85	*38.86*	38.71	*38.79*	38.72	*38.87*
ADR2	0 - 50 m	**38.36**	38.42	*38.49*	38.47	*38.52*	38.38	*38.44*	38.48	*38.40*	38.29	*38.37*	38.39	*38.63*
	50 - 100 m	**38.56**	38.59	*38.67*	38.65	*38.71*	38.57	*38.61*	38.66	*38.60*	38.45	*38.53*	38.54	*38.78*
	100 - 200 m	**38.60**	38.62	*38.68*	38.68	*38.75*	38.61	*38.64*	38.68	*38.64*	38.45	*38.55*	38.53	*38.80*
	200 - 500 m	**38.69**	38.72	*38.78*	38.77	*38.86*	38.73	*38.74*	38.77	*38.75*	38.55	*38.65*	38.61	*38.89*
	500 - 800 m	**38.78**	38.80	*38.87*	38.84	*38.96*	38.84	*38.84*	38.87	*38.87*	38.74	*38.81*	38.74	*38.87*
ION	0 - 50 m	**38.51**	38.39	*38.66*	38.44	*38.54*	38.47	*38.60*	38.38	*38.47*	38.29	*38.38*	38.47	*38.50*
	50 - 100 m	**38.55**	38.48	*38.68*	38.54	*38.63*	38.49	*38.67*	38.55	*38.62*	38.43	*38.51*	38.56	*38.73*
	100 - 200 m	**38.76**	38.82	*38.85*	38.83	*38.85*	38.77	*38.89*	38.89	*38.93*	38.68	*38.76*	38.79	*39.06*
	200 - 500 m	**38.86**	38.97	*38.94*	38.96	*38.96*	38.95	*38.99*	38.98	*39.00*	38.77	*38.85*	38.80	*39.06*
	500 - 800 m	**38.84**	38.91	*38.91*	38.91	*38.95*	38.92	*38.95*	38.93	*38.96*	38.86	*38.90*	38.81	*38.91*

Table 4 - Same as Table 3, for salinity.

Dataset and file format of physical variables

The original data from the two simulations have been processed as described in the previous sections. The resulting statistics have been organized in NetCDF files for the specific implementation of the integrated platform of WP4. The chosen standard (NetCDF) allows for a widespread use of the results in all FAIRSEA work packages. In fact, NetCDF (Network Common Data Form) files are self-describing (i.e., they include information about the data they contain), architecture-independent (i.e., they can be accessed by computers with different ways of storing integers, characters, and floating-point numbers), appendable (i.e., data can be easily appended to a NetCDF dataset) and sharable (i.e., multiple users can simultaneously access the same NetCDF file). NetCDF data can be browsed and analyzed through a number of software, like NCO, IDL, MATLAB, PYTHON, cdo, and ncl.

In the dataset, a section contains files named X_PERIOD_SCEN.nc, where X can be zonal (U) or meridional (V) component of speed, temperature (T) or salinity (S), PERIOD can be 2021-2025, 2026-2030, 2031-2040, 2040-2059 and 2080-2099 while SCEN is the scenario (RCP4.5 and RCP8.5). Each file contains the 2D annual anomaly for X between 0-50 m (for example anom_0m_50m), between 50-100 m (for example anom_50m_100m), between 100-200 m (for example anom_100m_200m), between 200-500 m (for example anom_200m_500m) and between 500-800 m (for example anom_500m_800m), its 2D standard deviation (for example std_0m_50m) and the 2D annual mean (for example mean_0m_50m) . The latter is defined as X_ANOM+X_REA where X_REA is the value of X already discussed in the deliverable of the present state 4.1.1 and 4.2.1 and available in the FAIRSEA repository. Each file has a dimension of 3 MB. Table 5 shows the dimensions and variables included in the NetCDF files.

SIZE	VARIABLES		
lon=144 lat=176	NAME	DIMENSIONS	TYPE
	Lon	lon	Float32
	Lat	lat	Float32
	mean_0m_50m	lat, lon	double
	mean_50m_100m	lat, lon	double
	mean_100m_200m	lat, lon	double
	mean_200m_500m	lat, lon	double
	mean_500m_800m	lat, lon	double
	anom_0m_50m	lat, lon	double
	anom_50m_100m	lat, lon	double
	anom_100m_200m	lat, lon	double
	anom_200m_500m	lat, lon	double
	anom_500m_800m	lat, lon	double
	std_0m_50m	lat, lon	double
	std_50m_100m	lat, lon	double
	std_100m_200m	lat, lon	double
	std_200m_500m	lat, lon	double
	std_500m_800m	lat, lon	double

Table 5 - Dimensions and variables included in the NetCDF files

The dataset consists also of a further section of files, named average_Xbottom.nc, where X can be temperature (T) or salinity (S) at the bottom. Each file contains again the 2D annual anomaly for X, its standard deviation and mean value computed as explained before at the bottom. Each file has a size of 0.7 MB. Table 6 shows the dimensions and variables included in these NetCDF files.

SIZE	VARIABLES		
lon=144 lat=176	**NAME**	**DIMENSIONS**	**TYPE**
	Lon	lon	Float32
	Lat	lat	Float32
	mean	lat, lon	double
	std	lat, lon	double
	anom	lat, lon	double

Table 6 - Dimensions and variables included in the NetCDF files

Acknowledgements

This report has been carried out with the contribution of Stefano Salon, Giorgio Bolzon and Paolo Lazzari (OGS) for the preparation and set up of the future scenario simulations, and for the implementation of the analysis protocol. We also thank Tomas Lovato (CMCC) for the preparation of the future hydrodynamic simulations runned at the CINECA supercomputing center.

References

Bethoux, J. P., Morin, P., Chaumery, C., Connan, O., Gentili, B., and Ruiz-Pino, D., 1998. Nutrients in the Mediterranean Sea, mass balance and statistical analysis of concentrations with respect to environmental change, Mar. Chem., 63, 155–169.

Cavicchia L., Gualdi S., Sanna A., Oddo P., 2015:" The Regional OceanAtmosphere Coupled Model COSMONEMO_MFS", CMCC Report, n RP0254, http://www.cmcc.it/publications/rp0254-the-regionalocean-atmosphere-coupled-model-cosmo-nemo_mfs

Cossarini G., Lazzari P., Solidoro, C., 2015. Spatiotemporal variability of alkalinity in the Mediterranean Sea. Biogeosciences, 12(6), 1647-1658.

Dee, D. P., S. M. Uppala, A. J. Simmons, P. Berrisford, P. Poli, S. Kobayashi, U. Andrae et al. "The ERA-Interim reanalysis: Configuration and performance of the data assimilation system." Quarterly Journal of the Royal Meteorological Society 137, no. 656 (2011): 553-597.

Emodnet, 2018. Mediterranean Sea - Eutrophication and Ocean Acidification aggregated datasets 1911/2017 v2018. Aggregated datasets were generated in the framework of EMODnet Chemistry III, under the support of DG MARE Call for Tender EASME/EMFF/2016/006 - lot4. Hellenic Centre for Marine Research, Hellenic National Oceanographic Data Centre (HCMR/HNODC) (2018). https://doi.org/10.6092/89576629-66D0-4B76-8382-5EE6C7820C7F

Foujols, M.-A., Lévy, M., Aumont, O., Madec, G., 2000. OPA 8.1 Tracer Model Reference Manual. Institut Pierre Simon Laplace, pp. 39.

Gualdi, S., Somot, S., Li, L., Artale, V., Adani, M., Bellucci, A., et al. (2013). The CIRCE simulations: Regional climate change projections with realistic representation of the mediterranean sea. *Bulletin of the American Meteorological Society, 94*, 65-81. doi:10.1175/BAMS-D-11-00136.1.

IPCC, 2014: AR5 Climate Change 2014: Synthesis Report. Contribution of Working Groups I, II and III to the Fifth Assessment Report of the Intergovernmental Panel on Climate Change.

Krom M.D., Kress N., Brenner S., Gordon L.I., 1991. Phosphorus limitation of primary productivity in the eastern Mediterranean Sea. Limnology and Oceanography, 36(3) 424-432.

Lazzari P., Teruzzi A., Salon S., Campagna S., Calonaci C., Colella S., Tonani M., Crise A. 2010. Pre-operational short-term forecasts for the Mediterranean Sea biogeochemistry. Ocean Science, 6, 25-39.

Lazzari, P., Solidoro, C., Ibello, V., Salon, S., Teruzzi, A., Béranger, K., Colella, S., and Crise, A., 2012. Seasonal and inter-annual variability of plankton chlorophyll and primary production in the Mediterranean Sea: a modelling approach. Biogeosciences, 9, 217-233.

Lazzari, P., Solidoro, C., Salon, S., Bolzon, G., 2016. Spatial variability of phosphate and nitrate in the Mediterranean Sea: a modelling approach. Deep Sea Research I, 108, 39-52.

Moss, R. H., Edmonds, J. A., Hibbard, K. A., Manning, M. R., Rose, S. K., Van Vuuren, D. P., Meehl, G. A. (2010). The next generation of scenarios for climate change research and assessment. Nature, 463(7282), 747-756.

Oddo, P., Adani, M., Pinardi, N., Fratianni, C., Tonani, M., & Pettenuzzo, D. (2009). A nested Atlantic-Mediterranean Sea general circulation model for operational forecasting. Ocean Science, 5, 461–473. https://doi.org/10.5194/os-5-461-2009.

Scoccimarro, E., S. Gualdi, A. Bellucci, A. Sanna, P. G. Fogli, E. Manzini, M. Vichi, P. Oddo, and A. Navarra (2011), Effects of tropical cyclones on ocean heat transport in a high resolution coupled general circulation model, J. Clim., 24, 4368– 4384, doi:10.1175/2011JCLI4104.1.

Teruzzi A., Dobricic S., Solidoro C., Cossarini G. 2013. A 3D variational assimilation scheme in coupled transport biogeochemical models: Forecast of Mediterranean biogeochemical properties, Journal of Geophysical Research, doi:10.1002/2013JC009277.

Thingstad T.F., Rassoulzadegan F., 1995. Nutrient limitations, microbial food webs, and 'biological C-pumps': suggested interactions in a P-limited Mediterranean. Marine Ecology Progress Series, 117: 299-306.